

Physics inspired priors for neutron star mergers improves equation of state constraints

SPENCER J. MAGNALL ,^{1,2} CHRISTIAN ECKER ,³ LUCIANO REZZOLLA ,^{3,4,5} AND PAUL D. LASKY ,^{1,2}

¹*School of Physics and Astronomy, Monash University, Clayton VIC 3800, Australia*

²*OzGrav: The ARC Centre of Excellence for Gravitational Wave Discovery, Clayton VIC 3800, Australia*

³*Institut für Theoretische Physik, Max-von-Laue-Strasse 1, 60438 Frankfurt, Germany*

⁴*Frankfurt Institute for Advanced Studies, Ruth-Moufang-Strasse 1, 60438 Frankfurt, Germany*

⁵*School of Mathematics, Trinity College, Dublin 2, Ireland*

ABSTRACT

Gravitational-wave astronomy shows great promise in determining nuclear physics in a regime not accessible to terrestrial experiments. We introduce physics-inspired priors informed by nuclear theory and perturbative quantum chromodynamics calculations as well as astrophysical measurements of neutron star masses and radii. When these priors are used in gravitational-wave astrophysical inference, we show significant improvement on nuclear equation of state constraints. Applying these to the first two gravitational-wave binary neutron star mergers GW170817 and GW190425, constraints on the radius of a $1.4 M_{\odot}$ neutron star improves from $R = \textcolor{red}{XX}_{-ZZ}^{+YY}$ km to $\textcolor{red}{XX}_{-ZZ}^{+YY}$ km (90% confidence intervals). We also show these priors can be used to perform model selection between binary neutron star and neutron star-black hole mergers, although the results for GW190425 are inconclusive with a Bayes factor of 1.33 in favour of the binary neutron star merger hypothesis, representing only marginal evidence. We advocate for these physics-inspired priors to be used as standard in the literature, and provide open-source code for reproducibility and further adaptation of the method. **CE:** The abstract seems a bit optimisitc. Can we actually claim an improvement of the NS EOS and radius constraints? **SM:** We should see some improvement compared to the LVK measurement as the posterior volume in $\mathcal{M} - \tilde{\Lambda}$ has decreased. Whether or not this improved constraint is significant when compared to the physics prior is less clear.

Keywords: neutron stars — gravitational waves — equation of state

1. INTRODUCTION

Some background sentences here on the importance and constraints of pQCD and nuclear theory.

When performing gravitational-wave astrophysical inference of binary neutron star mergers (e.g., Abbott et al. 2017, 2018, 2019, 2020), it is common to use ‘agnostic’ priors on their gravitational-wave observables, for example, uniform priors on chirp mass \mathcal{M} and the dimensionless tidal deformability parameter $\tilde{\Lambda}$. However, Altiparmak et al. (2022a); Ecker & Rezzolla (2022) showed that the above conditions imply highly correlated probability distributions in $\mathcal{M} - \tilde{\Lambda}$ parameter space.

In this work, we advocate using these physics-inspired priors joint priors on \mathcal{M} and $\tilde{\Lambda}$, which are the two best measured and most informative parameters related to the neutron star equation of state (EOS). We show an improvement on the measurement of the marginalized posterior on $\tilde{\Lambda}$ from the gravitational-wave observation

of GW170817 from $\tilde{\Lambda} = 466_{-158}^{+901}$ with the agnostic prior to $\tilde{\Lambda} = 384_{-226}^{+690}$ with the new physics-inspired prior. This corresponds to an improvement in the neutron star radius measurement of an equivalent $1.4 M_{\odot}$ star from $R_{1.4} = \dots$ **CE:** How to quantify this improvement?. **SM:** The easiest way is probably to compute 90% CI of mass-radius curves from the posteriors of both the official and physics inspired PE. We can then make a direct **R_{1.4} comparison**. For GW190425, the effective tidal deformability improves from $\tilde{\Lambda} = 381_{-110}^{+1446}$ to $\tilde{\Lambda} = 183_{-82}^{+362}$. **SM:** Do we constrain GW190425 relative to the BNS prior?

We also demonstrate the utility of these priors for distinguishing between the sources of Gravitational wave events. We perform model selection between a binary neutron star and neutron star – black hole origin of GW190425 and find a Bayes factor of 1.33 in favor of a binary neutron star origin.

In advocating for this prior becoming standard in the literature, we provide an open-source configuration for the BILBY Bayesian inference library (Ashton et al. 2019; Romero-Shaw et al. 2020) currently used for the majority of gravitational-wave parameter estimation by the LIGO-Virgo-KAGRA collaboration (Aasi et al. 2015; Acernese et al. 2015; Akutsu et al. 2020). This implements numerically the joint probability distribution as a constrained prior for \mathcal{M} and $\tilde{\Lambda}$ as described in the next section.

2. METHODS

Our setup closely follows that of Altiparmak et al. (2022b), which we briefly review here. We begin by constructing a large set of EOSs by stitching together various components. At the lowest densities ($n < 0.5 n_s$), with $n_s = 0.16 \text{ fm}^{-3}$ the nuclear saturation density, we adopt the Baym-Pethick-Sutherland (BPS) model (Baym et al. 1971) for the neutron-star crust. In the range $0.5 n_s < n < 1.1 n_s$, we randomly sample polytropes to span the range between the softest and stiffest EOSs from Hebeler et al. (2013). At high densities ($n \gtrsim 40 n_s$), corresponding to a baryon chemical potential of $\mu = 2.6 \text{ GeV}$, we impose the perturbative QCD constraint from Fraga et al. (2014) on the pressure $p(X, \mu)$ of cold quark matter, with the renormalization scale parameter X sampled uniformly in $[1, 4]$.

For the intermediate density range ($1.1 n_s < n \lesssim 40 n_s$), we use the parametrization method of Annala et al. (2020), which models the sound speed as a function of the chemical potential, $c_s^2(\mu)$, using piecewise-linear segments:

$$c_s^2(\mu) = \frac{(\mu_{i+1} - \mu) c_{s,i}^2 + (\mu - \mu_i) c_{s,i+1}^2}{\mu_{i+1} - \mu_i}, \quad (1)$$

where μ_i and $c_{s,i}^2$ are parameters defining the i -th segment in the range $\mu_i \leq \mu \leq \mu_{i+1}$. Throughout this work, we adopt natural units where $c = G = 1$.

The number density follows as

$$n(\mu) = n_1 \exp \left(\int_{\mu_1}^{\mu} \frac{d\mu'}{\mu' c_s^2(\mu')} \right), \quad (2)$$

where $n_1 = 1.1 n_s$, and $\mu_1 = \mu(n_1)$ is set by the corresponding polytrope EOS. The pressure is then obtained via

$$p(\mu) = p_1 + \int_{\mu_1}^{\mu} d\mu' n(\mu'), \quad (3)$$

where the integration constant p_1 matches the pressure of the polytrope at $n = n_1$. We numerically integrate Eq. (3) using seven segments for $c_s^2(\mu)$.

Using this framework, we generate $\approx 10^6$ EOSs by randomly selecting the maximum sound speed

$c_{s,\max}^2 \in [0, 1]$ and uniformly sampling the free parameters $\mu_i \in [\mu_1, \mu_{N+1}]$ (where $\mu_{N+1} = 2.6 \text{ GeV}$) and $c_{s,i}^2 \in [0, c_{s,\max}^2]$. These EOSs are by construction consistent with nuclear theory and perturbative QCD uncertainties.

To incorporate astrophysical constraints, we solve the Tolman-Oppenheimer-Volkoff (TOV) equations for each EOS and retain only those satisfying the mass measurements of J0348+0432 (Antoniadis et al. 2013) ($M = 2.01 \pm 0.04 M_\odot$) and J0740+6620 (Cromartie et al. 2020; Fonseca et al. 2021) ($M = 2.08 \pm 0.07 M_\odot$), discarding EOSs with a maximum mass $M_{\text{TOV}} < 2.0 M_\odot$. In addition, we impose NICER radius constraints from J0740+6620 (Miller et al. 2021; Riley et al. 2021) and J0030+0451 (Riley et al. 2019; Miller et al. 2019), rejecting EOSs with $R < 10.75 \text{ km}$ at $M = 2.0 M_\odot$ or $R < 10.8 \text{ km}$ at $M = 1.1 M_\odot$.

In the neutron star binary case, the binary tidal deformability is computed as

$$\tilde{\Lambda}_{\text{NSNS}} = \frac{16}{13} \frac{(12M_2 + M_1)M_1^4\Lambda_1 + (12M_1 + M_2)M_2^4\Lambda_2}{(M_1 + M_2)^5}, \quad (4)$$

where M_i , R_i , and $\Lambda_i = \frac{2}{3}k_2(R_i/M_i)^5$ ($i = 1, 2$) denote the component masses, radii, and tidal deformabilities, with k_2 being the second tidal Love number. The chirp mass is given by $\mathcal{M}_{\text{chirp}} = (M_1 M_2)^{3/5}(M_1 + M_2)^{-1/5}$ and we in the following we will use the mass ratio defined as $q = M_2/M_1$.

In the mixed binary case, i.e., where one binary component is a neutron star and the other one a black hole, the formula for the binary tidal deformability simplifies, because black holes have zero tidal deformability $\Lambda_{\text{BH}} = 0$. The binary tidal deformability in this case becomes

$$\tilde{\Lambda}_{\text{NSBH}} = \frac{16}{13} \frac{(12M_{\text{BH}} + M_{\text{NS}})M_{\text{NS}}^4\Lambda_{\text{NS}}}{(M_{\text{NS}} + M_{\text{BH}})^5}, \quad (5)$$

where M_{NS} and Λ_{NS} are the neutron star mass and tidal deformability, respectively, and M_{BH} the black hole mass. The expressions for the chirp mass and mass ratio remain intact, with the understanding that $M_1 = M_{\text{NS}}$ and $M_2 = M_{\text{BH}}$. Unlike in Altiparmak et al. (2022a); Ecker & Rezzolla (2022) we do not impose any GW informed constraints on the binary tidal deformability in the construction of our prior.

2.1. Binary neutron star mergers

We use the probability distributions of the previous section as priors on chirp mass and effective tidal deformability as shown in Fig. 1. We implement this in

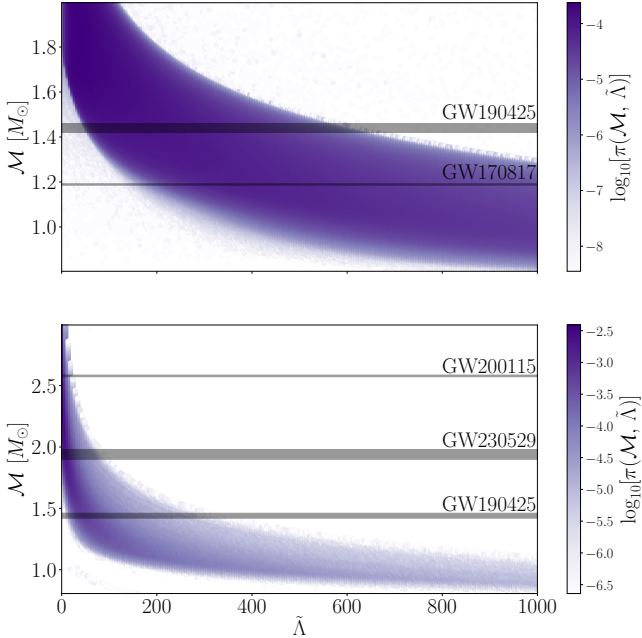


Figure 1. Coupled priors for the source-frame chirp mass \mathcal{M} and dimensionless tidal deformability $\tilde{\Lambda}$. Top: prior for binary neutron star mergers. Bottom: prior for neutron star – black hole mergers. The horizontal grey bands are the 90% credible intervals for the measured chirp masses of GW170817 (Abbott et al. 2017), GW190425 (Abbott et al. 2020), GW200115 (Abbott et al. 2021) and GW230529 (Abac et al. 2024).

BILBY using the `conditional_prior` function¹, interpolating the 200×200 grid to draw from a joint prior on \mathcal{M} and $\tilde{\Lambda}$.

We sample directly in source-frame chirp mass, mass ratio $q = m_1/m_2$ and the two tidal deformability parameters $\tilde{\Lambda}$ and $\delta\tilde{\Lambda}$ (see Favata 2014; Wade et al. 2014, for explicit expressions for these quantities). We note that q is not a variable that depends on the equation of state, but instead priors *could* be chosen based on astrophysical formation scenarios. In this work, we take the standard approach and choose a prior on q that is uniform between $q = 0.125$ and 1 (e.g., Romero-Shaw et al. 2020). We further note that, while both $\tilde{\Lambda}$ and $\delta\tilde{\Lambda}$ are related to the equation of state, we only impose a prior here on $\tilde{\Lambda}$. In general, $\tilde{\Lambda}$ is measured much better than $\delta\tilde{\Lambda}$, which can be understood because $\tilde{\Lambda}$ enters waveform approximates at the 5th post-Newtonian order, whereas $\delta\tilde{\Lambda}$ only enters at 6th in linear combination with $\tilde{\Lambda}$ (Wade et al. 2014). In principle, one could set a combined prior on the three parameters ($\mathcal{M}, \tilde{\Lambda}, \delta\tilde{\Lambda}$), however, adding this latter parameter would not add sig-

nificantly to parameter estimation in the relatively low signal-to-noise regime because of the above arguments.

2.2. Neutron star – black hole mergers

The parameterisation in the previous section does not go to high enough values of chirp mass because it is assumed both stars in the merger are neutron star. We therefore derive a new distribution for neutron star–black hole mergers by going back to the raw distributions of progenitor stellar masses and radii, and combining that progenitor with a black hole of mass m_1 and tidal deformability $\Lambda_1 = 0$. We use a uniform distributed mass ratio to generate our prior relationship. We have found more sophisticated mass-ratio distributions, such as those informed by state of the art binary population synthesis (e.g Broekgaarden et al. 2021) did not significantly impact the shape of the prior distribution. We demonstrate the independence of our results on the chosen population model in Appendix A. We choose once again to work with priors in $\mathcal{M} - \tilde{\Lambda}$, enforcing $\tilde{\Lambda}(\Lambda_2, \mathcal{M}, q)$ where Λ_2 is the tidal deformability of the lighter object in the binary, which we assume is the neutron star.

2.3. Parameter estimation

We perform Bayesian parameter estimation on the gravitational-wave strain data of the two (likely) binary neutron star merger events GW170817 and GW190425 using the strain data freely available from the GWOSC repository². We utilize the BILBY Bayesian inference framework and priors on source-frame chirp mass and tidal-deformability implemented in Section 2. Priors for all renaming parameters assume the low-spin ($\chi \leq 0.05$) defaults as defined in BILBY (e.g Ashton et al. 2019, Romero-Shaw et al. 2020).

Parameter estimation for each run was performed using the DYNESTY nested sampler (Speagle 2020) and the IMRPhenomPv2_NRTIDAL waveform (Dietrich et al. 2019). Analysis of binary neutron star merger signals is significantly computationally expensive and as such we utilize pBILBY (Smith et al. 2020), a parallel implementation of BILBY which uses the Message Passing Interface (MPI).

Since we are required to sample in the source-frame chirp mass instead of the observer frame, we must assume a cosmology. We use $H_0 = 67.66 \text{ km s}^{-1}$, $\Omega_M = 0.30966$ informed by the Planck 2018 results (Planck Collaboration et al. 2020).

We employ both the binary neutron star and the neutron star – black hole merger priors in our analysis of

¹ git link to our code!?

² <https://gwosc.org>

GW190425. This facilitates a model selection analysis between a binary neutron star, and neutron star – black hole origin of GW190425. The details of this model selection analysis are described further in Appendix B. For GW170817 we perform parameter estimation using the binary neutron star prior only.

We reconstruct mass–radius curves from posterior samples of source-frame chirp mass and tidal deformability by performing equation of state inference on the posterior samples of mass and tidal deformability. The posterior on the equation of state from the gravitational-wave data is

$$p(\epsilon|d) = \frac{p(d|\epsilon)\pi(\epsilon)}{\mathcal{Z}}, \quad (6)$$

where $\pi(\epsilon)$ is the prior on equation of state parameters ϵ , and \mathcal{Z} is the evidence. The likelihood is given by

$$\begin{aligned} p(d|\epsilon) \approx & \int dm_1 dm_2 p(m_1, m_2|\epsilon) \\ & \times p(d|m_1, m_2, \Lambda_1(\epsilon, m_1), \Lambda_2(\epsilon, m_2)), \end{aligned} \quad (7)$$

which is an integral over the binary masses m_1 and m_2 . We take the population priors on the mass distribution(s) for a given equation of state to be flat

$$p(m|\epsilon) = \begin{cases} \frac{1}{M_{\max} - M_{\min}}, & \text{if } M_{\min} \leq m \leq M_{\max}, \\ 0, & \text{else,} \end{cases} \quad (8)$$

where we set $M_{\min} = 1.0$ and $M_{\max} = M_{\text{TOV}}$. A flat mass distribution is a valid approximation as population parameters are not expected to significantly impact equation of state inference until $N \geq 20$ (e.g Agathos et al. 2015; Wysocki et al. 2020; Landry et al. 2020).

The second term in the integral is the likelihood obtained from the posterior samples of the gravitational-wave analysis. Which we obtain by marginalizing over nuisance parameters and dividing out the analysis priors.

3. RESULTS

Figure 2 shows the posterior distributions of intrinsic tidal parameter of GW170817 analyzed using the $\mathcal{M}-\tilde{\Lambda}$ feature (teal), when compared to the official posterior samples from the LVK (midnight blue). While we show only the tidal posteriors, we sample over all binary parameters. Posterior distributions for all other intrinsic and extrinsic binary parameters are identical.

Figure 3 shows the reconstructed mass–radius curves of GW170817 ...

Figure 4 shows the posterior distribution of the intrinsic tidal parameter of GW190425 when analyzed using both the binary neutron star prior (teal) and neutron

star – black hole prior (pink). We show the official posterior distribution of the LVK obtained using uniform priors in blue. Bayesian model selection between the binary neutron star and neutron star – black hole merger gives a Bayes factor of 1.33, marginally in favor of a binary neutron star merger origin. Figures 5 and 6 show the reconstructed mass–radius curves of GW190425 analyzed using the new priors.

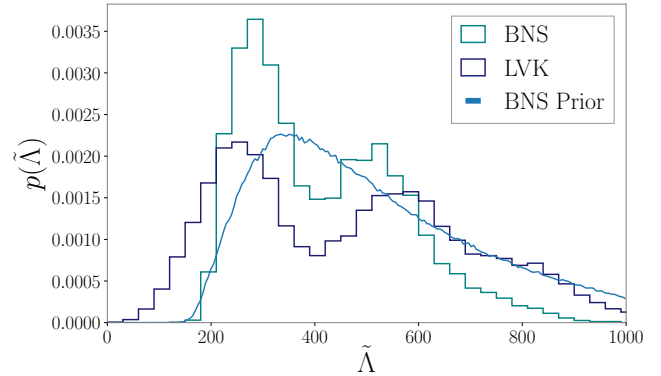


Figure 2. The posterior distributions of the tidal deformability $\tilde{\Lambda}$ obtained from Bayesian parameter estimation for GW170817. The posterior using a nuclear, microphysics, and astrophysics inspired prior is shown in teal, while the posterior using uniform priors from the LVK is shown in midnight blue. We show the (marginalized) prior with the light blue curve. Note, the posterior samples from the LVK show support up to $\tilde{\Lambda} = 2000$.

4. CONCLUSIONS

We have constructed new physics inspired priors for the analysis of gravitational-wave strain data of neutron star mergers. Analysis of the neutron star mergers GW170817 and GW190425 with our priors, constrains the effective tidal-deformability of GW170817 to $\tilde{\Lambda} = 384^{+690}_{-226}$ and GW190425 to $\tilde{\Lambda} = 183^{+362}_{-82}$. Corresponding to a 37%, and 80% decrease in the width of 90% credible interval respectively when compared to uniform priors. Performing equation of state inference, we find that the radius of a $1.4M_{\odot}$ neutron star can be constrained to XX at a 90% credible interval. Which suggests a preference for softer/stiffer equations of state ...

Model selection between a binary neutron star and neutron star – black hole origin on GW190425, yields marginal support for a binary neutron star origin. ...

In this work, we have constructed priors using binaries containing neutron stars with low spins ($\chi \leq 0.05$) only. However, analysis by the LVK typically involves both galactic “low-spin” and “high-spin” ($\chi \leq 0.89$) priors.

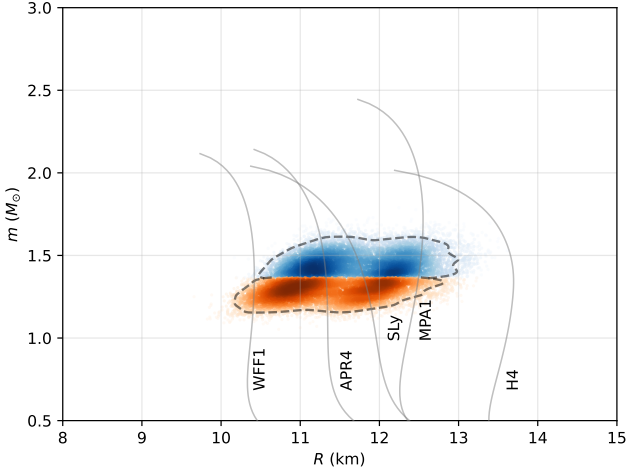


Figure 3. SM: These are some plots I generated using the YY universal relations so we can have a sense of the underlying EOS. Will replace with mass-radius curves when available. Posterior distributions of mass–radius for GW170817, analysed using the physics inspired BNS prior. The posterior distribution of the large neutron star is shown in blue, while the lighter neutron star is shown in orange. The dashed black line is the 90% CI, while the grey curves are representative tabulated equations of state.

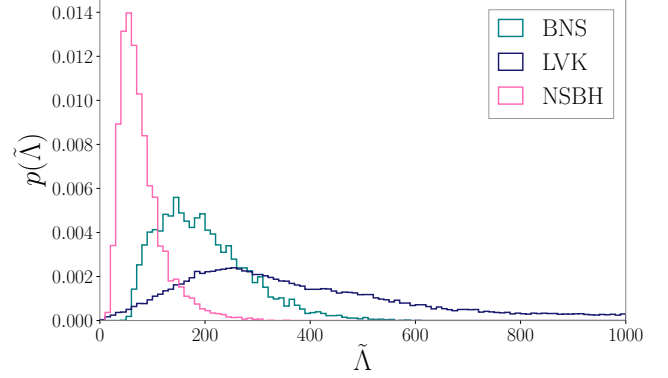


Figure 4. The posterior distributions of the tidal deformability $\tilde{\Lambda}$ obtained from Bayesian parameter estimation for G190425. The posterior using a nuclear, microphysics, and astrophysics inspired binary neutron star prior is shown in teal, and the corresponding neutron star – black hole prior is shown in pink. The posterior using uniform priors from the LVK is shown in midnight blue.

We leave the development of “high-spin” binary neutron star and neutron star – black hole priors to future work.

APPENDIX

A. NEUTRON STAR – BLACK HOLE MERGER PRIOR GENERATION

We should detail the prior generation for neutron star – black hole here, in particular the independence of a mass ratio informed by population synthesis on the prior distributions and potentially the resultant posterior distributions. Might be worth showing an extreme example to prove the point.

We generate two relations, one with uniform priors on our population of BH - NS mergers, and one directly informed by state of the art binary population synthesis. We use the mass ratio distribution of Broekgaarden et al. (2021) ([what particular model are we using?](#)) for the generation of our population synthesis informed priors. Figure 7 shows the distribution in mass ratio used for the generation of the prior.

B. MODEL SELECTION

We perform parameter estimation of gravitational-wave strain data using the DYNESTY nested sampler. Unlike standard MCMC samplers, DYNESTY calculates the evidence for each parameter estimation run. To perform Bayesian model selection between binary neutron star and neutron star– black hole mergers, we calculate the Bayes factor

$$BF_{\text{NSBH}}^{\text{BNS}} = \frac{\mathcal{Z}_{\text{BNS}}}{\mathcal{Z}_{\text{NSBH}}}, \quad (\text{B1})$$

where \mathcal{Z}_{BNS} and $\mathcal{Z}_{\text{NSBH}}$ are the Bayesian evidences obtained for the parameter estimation runs using the binary neutron star and neutron star black hole priors respectively. Formally, for model selection we should be computing the odds ratio, which is defined as

$$\mathcal{O}_{\text{NSBH}}^{\text{BNS}} \equiv \frac{\mathcal{Z}_{\text{BNS}}}{\mathcal{Z}_{\text{NSBH}}} \frac{\pi_{\text{BNS}}}{\pi_{\text{NSBH}}}, \quad (\text{B2})$$

where π_{BNS} and π_{NSBH} are the prior odds for each hypothesis; i.e our relative belief about which hypothesis is more likely. In this work we set the prior odds to unity, so the odds ratio is the Bayes factor. We could in principle construct an odds ratio where the prior odds was informed by the relative rates of binary neutron star and neutron – star black

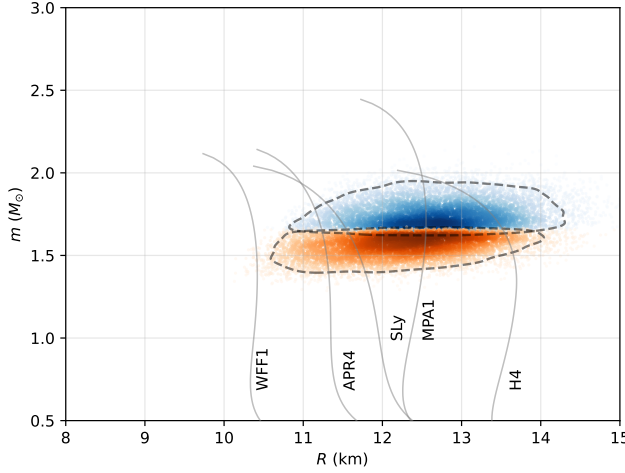


Figure 5. Posterior distributions of mass–radius for GW190425, analysed using the physics inspired BNS prior. The posterior distribution of the large neutron star is shown in blue, while the lighter neutron star is shown in orange. The dashed black line is the 90% CI, while the grey curves are representative tabulated equations of state.

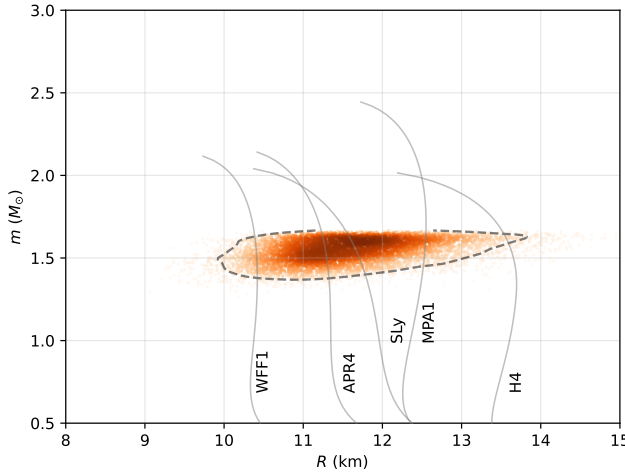


Figure 6. Posterior distributions of mass–radius for GW190425, analysed using the physics inspired NSBH prior. The posterior distribution of the large neutron star is shown in blue, while the lighter neutron star is shown in orange. The dashed black line is the 90% CI, while the grey curves are representative tabulated equations of state.

hole mergers. However since these rates are still highly uncertain, we choose the more agnostic approach of setting the prior odds to unity.

REFERENCES

Aasi, J., Abbott, B. P., Abbott, R., et al. 2015, Classical and Quantum Gravity, 32, 074001,
doi: [10.1088/0264-9381/32/7/074001](https://doi.org/10.1088/0264-9381/32/7/074001)

Abac, A. G., Abbott, R., Abouelfettouh, I., et al. 2024,
ApJL, 970, L34, doi: [10.3847/2041-8213/ad5beb](https://doi.org/10.3847/2041-8213/ad5beb)

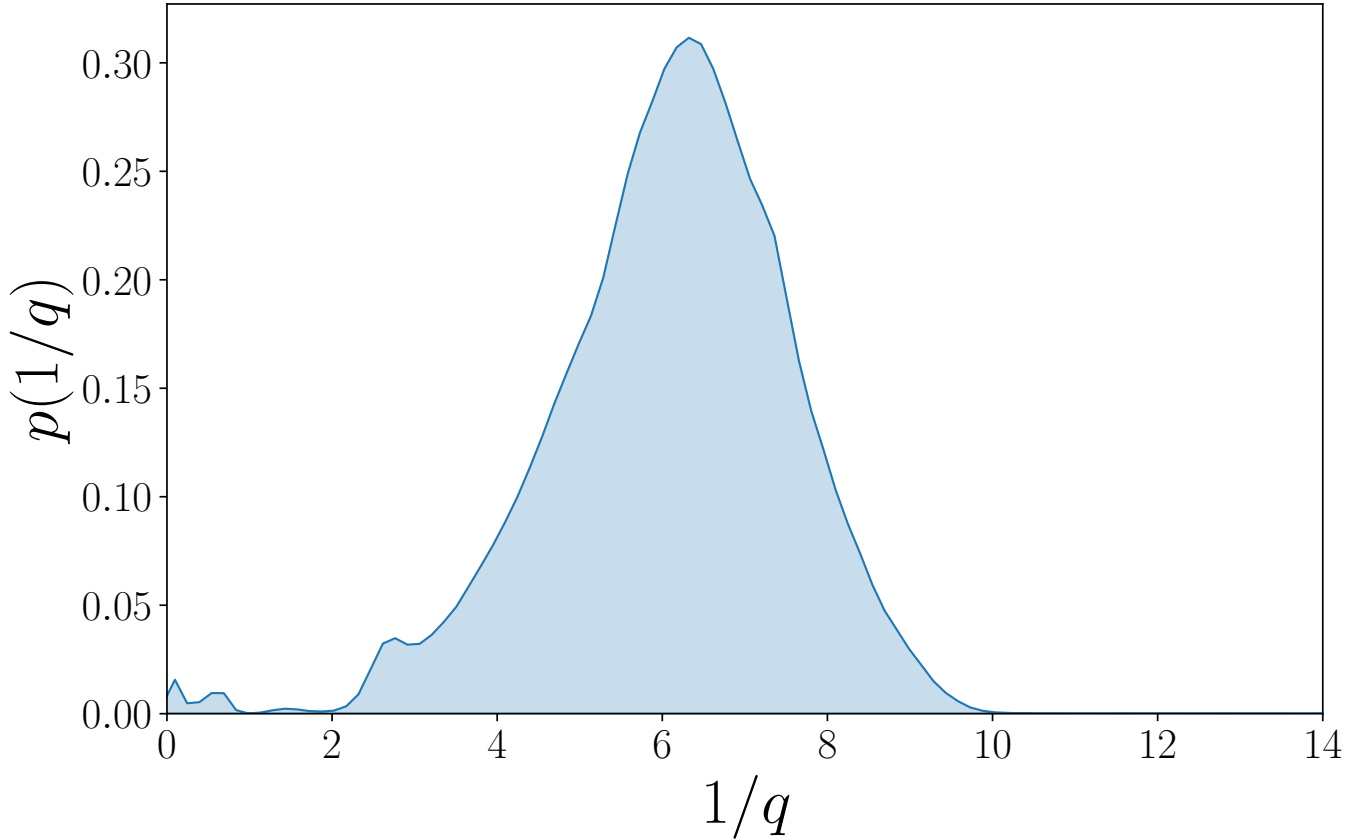


Figure 7. Probability density function of the mass ratio for detectable neutron star black hole mergers from (Broekgaarden et al. 2021).

- Abbott, B. P., Abbott, R., Abbott, T. D., et al. 2017, PhRvL, 119, 161101,
doi: [10.1103/PhysRevLett.119.161101](https://doi.org/10.1103/PhysRevLett.119.161101)
- . 2018, PhRvL, 121, 161101,
doi: [10.1103/PhysRevLett.121.161101](https://doi.org/10.1103/PhysRevLett.121.161101)
- . 2019, Physical Review X, 9, 011001,
doi: [10.1103/PhysRevX.9.011001](https://doi.org/10.1103/PhysRevX.9.011001)
- . 2020, ApJL, 892, L3, doi: [10.3847/2041-8213/ab75f5](https://doi.org/10.3847/2041-8213/ab75f5)
- Abbott, R., Abbott, T. D., Abraham, S., et al. 2021, ApJL, 915, L5, doi: [10.3847/2041-8213/ac082e](https://doi.org/10.3847/2041-8213/ac082e)
- Acernese, F., Agathos, M., Agatsuma, K., et al. 2015, Classical and Quantum Gravity, 32, 024001,
doi: [10.1088/0264-9381/32/2/024001](https://doi.org/10.1088/0264-9381/32/2/024001)
- Agathos, M., Meidam, J., Del Pozzo, W., et al. 2015, PhRvD, 92, 023012, doi: [10.1103/PhysRevD.92.023012](https://doi.org/10.1103/PhysRevD.92.023012)
- Akutsu, T., Ando, M., Arai, K., et al. 2020, Progress of Theoretical and Experimental Physics, 2021, 05A101,
doi: [10.1093/ptep/ptaa125](https://doi.org/10.1093/ptep/ptaa125)
- Altiparmak, S., Ecker, C., & Rezzolla, L. 2022a, ApJL, 939, L34, doi: [10.3847/2041-8213/ac9b2a](https://doi.org/10.3847/2041-8213/ac9b2a)
- . 2022b, Astrophys. J. Lett., 939, L34,
doi: [10.3847/2041-8213/ac9b2a](https://doi.org/10.3847/2041-8213/ac9b2a)
- Annala, E., Gorda, T., Kurkela, A., Näättilä, J., & Vuorinen, A. 2020, Nature Physics, 16, 907,
doi: [10.1038/s41567-020-0914-9](https://doi.org/10.1038/s41567-020-0914-9)
- Antoniadis, J., Freire, P. C. C., Wex, N., et al. 2013, Science, 340, 448, doi: [10.1126/science.1233232](https://doi.org/10.1126/science.1233232)
- Ashton, G., Hübner, M., Lasky, P. D., et al. 2019, ApJS, 241, 27, doi: [10.3847/1538-4365/ab06fc](https://doi.org/10.3847/1538-4365/ab06fc)
- Baym, G., Pethick, C., & Sutherland, P. 1971, ApJ, 170, 299, doi: [10.1086/151216](https://doi.org/10.1086/151216)
- Broekgaarden, F. S., Berger, E., Neijssel, C. J., et al. 2021, MNRAS, 508, 5028, doi: [10.1093/mnras/stab2716](https://doi.org/10.1093/mnras/stab2716)
- Cromartie, H. T., Fonseca, E., Ransom, S. M., et al. 2020, Nature Astronomy, 4, 72, doi: [10.1038/s41550-019-0880-2](https://doi.org/10.1038/s41550-019-0880-2)
- Dietrich, T., Samajdar, A., Khan, S., et al. 2019, PhRvD, 100, 044003, doi: [10.1103/PhysRevD.100.044003](https://doi.org/10.1103/PhysRevD.100.044003)
- Ecker, C., & Rezzolla, L. 2022, Mon. Not. Roy. Astron. Soc., 519, 2615, doi: [10.1093/mnras/stac3755](https://doi.org/10.1093/mnras/stac3755)
- Favata, M. 2014, PhRvL, 112, 101101,
doi: [10.1103/PhysRevLett.112.101101](https://doi.org/10.1103/PhysRevLett.112.101101)
- Fonseca, E., Cromartie, H. T., Pennucci, T. T., et al. 2021, Astrophys. J. Lett., 915, L12,
doi: [10.3847/2041-8213/ac03b8](https://doi.org/10.3847/2041-8213/ac03b8)

- Fraga, E. S., Kurkela, A., & Vuorinen, A. 2014, ApJL, 781, L25, doi: [10.1088/2041-8205/781/2/L25](https://doi.org/10.1088/2041-8205/781/2/L25)
- Hebeler, K., Lattimer, J. M., Pethick, C. J., & Schwenk, A. 2013, Astrophys. J., 773, 11, doi: [10.1088/0004-637X/773/1/11](https://doi.org/10.1088/0004-637X/773/1/11)
- Landry, P., Essick, R., & Chatzioannou, K. 2020, PhRvD, 101, 123007, doi: [10.1103/PhysRevD.101.123007](https://doi.org/10.1103/PhysRevD.101.123007)
- Miller, M. C., Lamb, F. K., Dittmann, A. J., et al. 2019, Astrophys. J. Lett., 887, L24, doi: [10.3847/2041-8213/ab50c5](https://doi.org/10.3847/2041-8213/ab50c5)
- . 2021, Astrophys. J. Lett., 918, L28, doi: [10.3847/2041-8213/ac089b](https://doi.org/10.3847/2041-8213/ac089b)
- Planck Collaboration, et al. 2020, A&A, 641, A6, doi: [10.1051/0004-6361/201833910](https://doi.org/10.1051/0004-6361/201833910)
- Riley, T. E., Watts, A. L., Bogdanov, S., et al. 2019, Astrophys. J. Lett., 887, L21, doi: [10.3847/2041-8213/ab481c](https://doi.org/10.3847/2041-8213/ab481c)
- Riley, T. E., Watts, A. L., Ray, P. S., et al. 2021, Astrophys. J. Lett., 918, L27, doi: [10.3847/2041-8213/ac0a81](https://doi.org/10.3847/2041-8213/ac0a81)
- Romero-Shaw, I. M., Talbot, C., Biscoveanu, S., et al. 2020, MNRAS, 499, 3295, doi: [10.1093/mnras/staa2850](https://doi.org/10.1093/mnras/staa2850)
- Smith, R. J. E., Ashton, G., Vajpeyi, A., & Talbot, C. 2020, MNRAS, 498, 4492, doi: [10.1093/mnras/staa2483](https://doi.org/10.1093/mnras/staa2483)
- Speagle, J. S. 2020, MNRAS, 493, 3132, doi: [10.1093/mnras/staa278](https://doi.org/10.1093/mnras/staa278)
- Wade, L., Creighton, J. D. E., Ochsner, E., et al. 2014, PhRvD, 89, 103012, doi: [10.1103/PhysRevD.89.103012](https://doi.org/10.1103/PhysRevD.89.103012)
- Wysocki, D., O'Shaughnessy, R., Wade, L., & Lange, J. 2020, arXiv e-prints, arXiv:2001.01747, doi: [10.48550/arXiv.2001.01747](https://doi.org/10.48550/arXiv.2001.01747)